Determination of the Fermi Surface of MgB_2 by the de Haas–van Alphen Effect

A. Carrington,[1] P. J. Meeson,[1] J. R. Cooper,[2] L. Balicas,[3] N. E. Hussey,[1] E. A. Yelland,[2] S. Lee,[4] A. Yamamoto,[4] S. Tajima,[4] S. M. Kazakov,[5] and J. Karpinski[5]

[1]*H. H. Wills Physics Laboratory, University of Bristol, Tyndall Avenue, Bristol BS8 1TL, United Kingdom*
[2]*Interdisciplinary Research Centre in Superconductivity and Department of Physics, University of Cambridge, Madingley Road, Cambridge CB3 0HE, United Kingdom*
[3]*National High Magnetic Field Laboratory, Florida State University, Tallahassee, Florida 32306, USA*
[4]*Superconductivity Research Laboratory, International Superconducting Technology Center, Tokyo 135-0062, Japan*
[5]*Laboratorium für Festkörperphysik, ETH Zürich, CH-8093 Zürich, Switzerland*

(Received 18 April 2003; published 17 July 2003)

We report measurements of the de Haas–van Alphen (dHvA) effect for single crystals of MgB_2, in magnetic fields up to 32 T. In contrast to our earlier work, dHvA orbits from all four sheets of the Fermi surface were detected. Our results are in good overall agreement with calculations of the electronic structure and the electron-phonon mass enhancements of the various orbits, but there are some small quantitative discrepancies. In particular, systematic differences in the relative volumes of the Fermi-surface sheets and the magnitudes of the electron-phonon coupling constants could be large enough to affect detailed calculations of T_c and other superconducting properties.

DOI: 10.1103/PhysRevLett.91.037003 PACS numbers: 74.25.Jb, 74.70.Ad

Since the recent discovery [1] of superconductivity at 39 K in MgB_2, there has been rapid progress in understanding its physical properties. The accepted consensus is that it is an *s*-wave, phonon-mediated superconductor but with some highly unusual properties. The most important of these are the anomalously high T_c and the existence of two, almost distinct, superconducting gaps. This understanding is based on many experiments and on theoretical calculations of the unusual electronic structure of MgB_2 [2–5].

There have been two direct experimental probes of the Fermi-surface (FS) structure of MgB_2; angle-resolved photoemission spectroscopy (ARPES) [6] and the de Haas–van Alphen effect (dHvA) [7]. The ARPES study showed band dispersions mostly in good agreement with theory, but the lack of k_z resolution precluded identification of one of the four bands. Moreover, ARPES has not yet been able to provide detailed information on the size of the Fermi-surface sheets or the mass enhancements. Our previous dHvA study [7] showed good agreement between theory and experiment regarding the areas of the orbits that were observed and their electron-phonon mass enhancements. However, only three out of nine predicted dHvA orbits were observed (labeled 1, 2, and 3 in Fig. 1) and so information was only obtained about two of the four FS sheets predicted by band calculations. It was not entirely clear whether the unobserved orbits were missing simply because of their relatively short mean-free paths, or whether the topology of the other sheets was substantially different. This issue clearly affects calculations of many physical properties (especially T_c). In this Letter, we report new measurements of the dHvA effect in magnetic fields up to 32 T for two single crystals. These new results give evidence for orbits on all four sheets of the Fermi surface.

Experiments were conducted on two different crystals grown by different groups. Sample *B* is one of the crystals studied previously [7] and was grown in Tokyo by high pressure synthesis using natural boron. Sample *K* was grown in Zürich by a similar technique but isotopically pure boron-10 was used as a starting ingredient [8]. Other crystals from the same batches were found to have T_c (onset) of 38.0 and 37.7 K for the Tokyo and Zürich crystals, respectively. dHvA oscillations were observed by measuring the torque (Γ) with a piezoresistive cantilever technique [9]. Both samples were studied extensively at Bristol in fields up to 20.5 T and temperatures down to 0.3 K, and in fields up to 32 T at the National High Magnetic Field Laboratory.

The first harmonic of the oscillatory part of the torque for a 3D Fermi liquid is given by [10,11]

$$\Gamma_{\mathrm{osc}} \propto \frac{1}{C}\frac{dF}{d\theta} B^{1/2} R_D R_T R_S \sin\left(\frac{2\pi F}{B} + \gamma\right), \qquad (1)$$

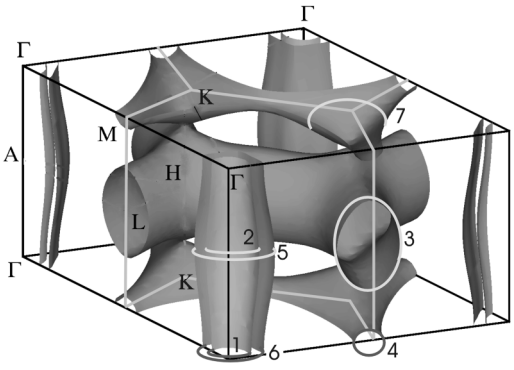

FIG. 1. Calculated Fermi surface topology, with possible dHvA extremal orbits (for frequencies <10 kT) indicated. This figure was adapted from Kortus *et al.* [2].

where F is the dHvA frequency [$F = (\hbar/2\pi e)A$, and A is the extremal orbit area in $\mathbf{k}$ space]; C is the curvature factor, and γ is the phase; R_D, R_T, and R_S are the damping factors from impurity scattering, temperature, and spin splitting, respectively. The Dingle factor, $R_D = \exp(-\pi m_B/eB\tau)$, where m_B is the unenhanced band mass [10,11] and τ is the scattering time. An equivalent expression for R_D is $R_D = \exp(-\pi\hbar k_F/eB\ell)$, which shows clearly the increased damping with a shorter mean-free path ℓ and increased average Fermi wave vector (k_F) of the orbit. $R_T = X/(\sinh X)$, where $X = (2\pi^2 k_B/\hbar e)(m^* T/B)$, and m^* is the quasiparticle effective mass. Finally, the spin splitting factor is given by $R_S = \cos[\pi n g m_B(1 + S)/2m_e]$, where $(1 + S)$ is the orbitally averaged exchange-correlation (Stoner) enhancement factor, g is the electron g factor, m_e is the free-electron mass, and n is an integer.

The electronic structure and dHvA orbits of MgB_2 have been calculated by three different groups [12–14]. The calculated Fermi surface is shown in Fig. 1, together with the expected dHvA extremal orbits [15]. The calculations [2] show that the electronic states near the Fermi level arise primarily from the boron atomic orbitals. The calculated Fermi surface is composed of four distinct sheets. Two of these arise from boron σ orbitals and are quasi-two-dimensional warped cylinders running along the c direction, whereas the other two are tubular networks with larger c-axis dispersion that are mainly formed from the boron π orbitals. In total nine primary extremal orbits have been predicted, and seven of these are labeled in the figure (two orbits with frequencies $>$ 30 kT have been omitted). Calculations of the dHvA frequencies and masses of the various orbits by the three groups are all in good agreement (the differences are typically 100–200 T, and $\lesssim 5\%$, respectively).

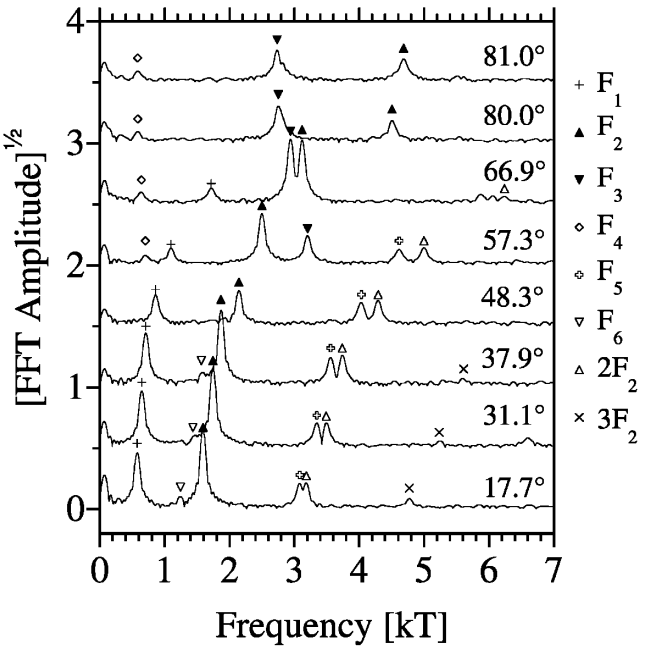

FIG. 2. Fourier transforms of the raw high field data for crystal K at 1.4 K and fields from 20–32 T. (The square root of the FFT amplitude is plotted and the data are offset for clarity.) The orbit assignments are indicated by symbols and follow the notation of Fig. 1

The fast Fourier transforms (FFTs) of the raw torque data between 20 and 32 T at 1.4 K for crystal K are shown in Fig. 2, as a function of angle θ as the sample was rotated from $H \parallel c$ to $H \parallel a$ ($H \parallel c \equiv 0°$). In addition to the frequencies observed in our previous study [7] (F_1, F_2, and F_3), several additional peaks are visible. Some care is needed in interpreting these new frequencies. Because the cantilever is deflected slightly by the torque, the torque measurements are not made at constant angle. This generates spurious harmonics and combinations of the main dHvA oscillations. For crystal K only weak harmonics of F_2 are observed (just above F_5—see Fig. 2), while for the larger crystal B, several harmonics of F_3 and a frequency corresponding to $F_1 + F_2$ were observed.

The observed frequencies (omitting those assigned as harmonics or combinations) are shown in Fig. 3 as a function of θ for both crystals. The solid lines in Fig. 3 are fits of the observed $F(\theta)$ values to $F(\theta) = \sum_{i=1}^{3} a_i/\cos^i(\theta - \theta_0)$ ($\theta_0 = 0$ or 90°), which we use to extrapolate the observed frequencies to the symmetry points (we denote these frequencies as F_n^0). The assignment of the FFT peaks to the orbits shown in Fig. 1 was achieved by comparing the values of the frequencies obtained by extrapolation, and their angular dependencies, with the calculations.

For crystal K, signals from six orbits associated with all four sheets of Fermi surface are observed. We are therefore able to verify experimentally the Fermi-surface topology predicted by Kortus *et al.* [2] and shown in Fig. 1. For crystal B, in addition to the three orbits observed previously, three further frequencies are seen. One of these can be assigned to F_4. The frequency of F_3^* ($F = 4600$ T) is close to that predicted for orbit 7 ($F = 4294$ T) [12] (and has a similar effective mass), however, the frequency is also close to that expected for an orbit equivalent to F_3 but from the tube oriented along a^* (i.e., at 60° to a). A subsequent in-plane rotation study showed the latter to be the most likely origin. The origin of F_{3S} is less clear, but it could arise from a slight warping of the same in-plane tube responsible for F_3.

Table I shows that the values of F^0 found for the two crystals are in good agreement. In total, we have studied crystals from six batches (five from Tokyo and one from Zürich) and so far, the dHvA frequencies agree to within 30 T or 0.06% of the basal area of the first Brillouin zone [$(\hbar/2\pi e)(8\pi^2/\sqrt{3}a^2) = 50.2$ kT]. This suggests that although T_c is slightly reduced compared with the best polycrystalline samples, any possible Mg deficiency is very reproducible and probably small [16].

The differences between the measured F^0 values and those predicted by theory are significant fractions of F^0

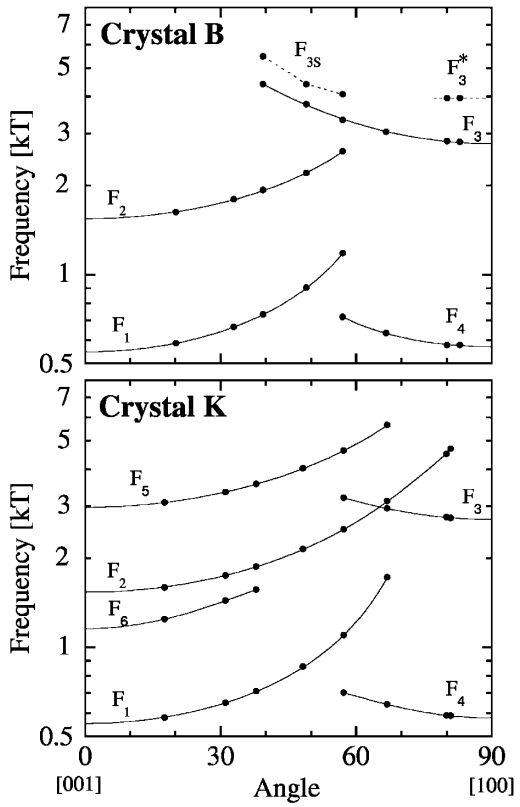

FIG. 3. Observed frequencies versus angle as the samples were rotated from $H \parallel c$ to (approximately) $H \parallel a$. The solid lines are polynomial fits to the data as described in the text, and the dotted lines are guides to the eye.

in some cases; however, a discrepancy of 100 T only amounts to ~0.3% of the basal area of the Brillouin zone. The volumes of the c-axis tubes are proportional to the average of the two extremal areas [14] and these are both ~16% smaller than the calculations [13], implying a corresponding reduction in the number of holes in these two tubes [14]. This may have a significant effect on calculations of physical properties.

It is instructive [13,14] to calculate the Fermi energy shift ΔE which would bring the theoretical frequencies in line with experiment. As the dHvA band mass is defined as $m_B = (\hbar^2/2\pi)(\partial A/\partial E)$, the necessary band shifts are given by $\Delta E = (\hbar e/m_B)\Delta F$ (where $\Delta F = F_{\mathrm{Th}} - F_{\mathrm{exp}}$). There is remarkable consistency between the ΔE values for the orbits, with the values roughly falling into two groups (Table I). For the σ sheet orbits (1, 2, 5, 6) the average shift is 83 ± 4 meV, whereas for the π sheet orbits (3, 4) it is -61 ± 5 meV. Because of the high degree of reproducibility of the frequencies between samples, it is unlikely that this discrepancy is caused by sample impurities or nonstoichiometry. Instead, it seems to imply a shortcoming of the local density approximation calculations [13,14].

Quasiparticle effective masses were determined by performing field sweeps at different temperatures and fitting the amplitudes to Eq. (1). Our experimental values of m^* are compared with the calculated band masses in Table I. In MgB_2 the dominant source of mass enhancement is the electron-phonon interaction. If we assume this is the only source of enhancement we can calculate an upper bound for the electron-phonon coupling constants λ^{ep}, from $\lambda^{\mathrm{ep}} = m^*/m_B - 1$. The results (Table I) show that the values of λ^{ep} on *both* the σ sheets are approximately a factor 3 larger than those on the π sheets.

A detailed comparison with the orbit-resolved theoretical values [13] of λ^{ep} is also shown in the table. Generally our values are slightly smaller than the theoretical ones. The most significant differences are for the larger orbits on the σ tubes for which the λ^{ep} values are ~20% smaller than theory. The small shifts in Fermi level described above do make small differences to the calculated band masses [13], increasing the $\lambda^{\mathrm{ep}}_{\mathrm{exp}}$ values by ~6%, but the differences remain significant and could have a relatively large effect on the detailed calculations of T_c. For example, using the isotropic McMillan equation, with parameters appropriate to MgB_2 [4] we estimate a 20% reduction in λ^{ep} would imply an 8 K reduction in T_c. It is likely that the reduced λ values we observe are caused by phonon anharmonicity, which has been shown to reduce the average value of λ by around 20% [4].

The mean free path ℓ on several orbits could be calculated by fitting the raw torque versus field data to Eq. (1) (see Table I). It can be seen that ℓ for sample K is significantly longer for orbits F_2 and F_1 on the c-axis tube but not for F_3 on the in-plane tubular network. The reason for this is not clear, but it does not necessarily indicate a higher crystal quality. However, F_5 and F_6 are

TABLE I. Summary of dHvA parameters for both samples (K and B) along with the theoretical predictions (Th) [13].

		Crystal K									Crystal B			
Orbit		F^0_{exp} (T)	F_{Th} (T)	ΔF (T)	ΔE (meV)	ℓ (Å)	m^*_{exp} (m_e)	m_{band} (m_e)	$\lambda^{\mathrm{ep}}_{\mathrm{exp}}$	$\lambda^{\mathrm{ep}}_{\mathrm{Th}}$	F^0_{exp} (T)	ℓ (Å)	m^*_{exp} (m_e)	$\lambda^{\mathrm{ep}}_{\mathrm{exp}}$
1	σ	551	730	+179	+83	550	0.548 ± 0.02	0.251	1.18 ± 0.1	1.25	546	380	0.553 ± 0.01	1.20 ± 0.04
2	σ	1534	1756	+222	+82	900	0.610 ± 0.01	0.312	0.96 ± 0.03	1.25	1533	580	0.648 ± 0.01	1.08 ± 0.03
3	π	2705	2889	+184	−67	570	0.439 ± 0.01	0.315	0.40 ± 0.03	0.47	2685	680	0.441 ± 0.01	0.40 ± 0.03
4	π	576	458	−118	−56	···	0.31 ± 0.05	0.246	0.31 ± 0.1	0.43	553	···	0.35 ± 0.02	0.42 ± 0.08
5	σ	2971	3393	+422	+79	390	1.18 ± 0.04	0.618	0.91 ± 0.07	1.16	···	···	···	···
6	σ	1180	1589	+409	+87	···	1.2 ± 0.1	0.543	1.2 ± 0.2	1.16	···	···	···	···

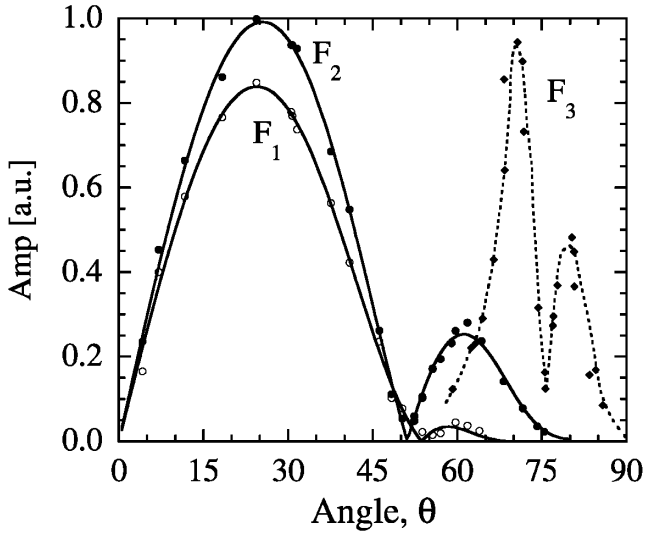

FIG. 4. FFT amplitude versus angle for frequencies F_1, F_2, and F_3 in crystal K. The solid lines are fits to the data as described in the text. The dotted line is a guide to the eye.

almost certainly observable in crystal K because of the larger values of ℓ for the two c-axis σ tubes. These differences in ℓ may be at least partially responsible for a significant difference in the B_{c2} values for the two crystals. For crystal B, $B_{c2}^{\|c} = 3.3$ T, $B_{c2}^{\perp c} = 17$ T, and for crystal K, $B_{c2}^{\|c} = 2.5$ T, $B_{c2}^{\perp c} = 12$ T (all values quoted at $T = 0.3$ K).

The longer mean free path of the smaller σ tube (F_1 and F_2) in crystal K has allowed us to track the amplitude of the signal over a very wide range of angle (up to 67° and 81°, respectively). The data shown in Fig. 4 show pronounced minima at $\theta = 51 \pm 1°$, $\theta = 53 \pm 1°$, $\theta = 75.7 \pm 0.5°$ for F_1, F_2, and F_3, respectively, which we attribute to the spin-zero effect [the R_s damping term in Eq. (1)]. Using the calculations of $m_B(\theta)$ by Harima [12] we can deduce the enhancement of the spin susceptibility $(1 + S)$ for these three orbits (at the spin-zero angle). Taking $g = 2$, we find that $S = 0.07$, 0.12, and 0.45 for the three orbits, respectively. The reason for the significantly larger enhancement on the π band is not clear. Band structure calculations [13] predict $S = 0.31$ and 0.26 on the F_2 and F_3 orbits, respectively. The calculation therefore overestimates S on the σ sheet by a factor 2.5 and underestimates it on the π sheet by a factor 1.7.

The solid lines in Fig. 4 show a fit to the data for F_1 and F_2 with Eq. (1), using the $m_B(\theta)$ values of Harima [12]. There are three free parameters: the overall amplitude, τ^{-1} (assumed constant as a function of angle), and S. The fit is remarkably good and the values of ℓ were found to be 410 and 900 Å for F_1 and F_2, respectively, which are close to the values obtained from the Dingle plots (see Table I). However, it was not possible to fit the data for F_3 because the abrupt fall for $\theta \lesssim 68°$ cannot be explained simply in terms of the angular dependence of m_B and a constant scattering rate (Dingle plots show that τ is approximately constant with angle).

In conclusion, our data strongly support the overall topology of the predicted electronic structure of MgB_2 and the calculations of the electron-phonon coupling constants for the different orbits. Our data give direct evidence that the electron-phonon interaction is large on *both* σ sheets and much smaller on *both* π sheets. We have therefore obtained conclusive evidence in favor of the two key ingredients in the two-gap model of superconductivity in this compound, namely, the Fermi-surface topology and the disparity in the electron-phonon coupling for the σ and π bands.

We thank a number of people for useful conversations and insights: N. W. Ashcroft, S. L. Drechsler, H. Harima, S. M. Hayden, and I. I. Mazin. This work was supported by the EPSRC (U.K.), NEDO (Japan), and the NSF through Grant No. NSF-DMR-0084173. We also thank R. Wiltshire for technical assistance.

[1] J. Nagamatsu *et al.*, Nature (London) **410**, 63 (2001).
[2] J. Kortus, I. I. Mazin, K. D. Belashchenko, V. P. Antropov, and L. L. Boyer, Phys. Rev. Lett. **86**, 4656 (2001).
[3] A. Y. Liu, I. I. Mazin, and J. Kortus, Phys. Rev. Lett. **87**, 087005 (2001).
[4] H. J. Choi *et al.*, Nature (London) **418**, 758 (2002); Phys. Rev. B **66**, 020513(R) (2002).
[5] I. I. Mazin *et al.*, Phys. Rev. Lett. **89**, 107002 (2002).
[6] H. Uchiyama *et al.*, Phys. Rev. Lett. **88**, 157002 (2002).
[7] E. A. Yelland, J. R. Cooper, A. Carrington, N. E. Hussey, P. J. Meeson, S. Lee, A. Yamamoto, and S. Tajima, Phys. Rev. Lett. **88**, 217002 (2002).
[8] Raman studies of crystals from the same batch give a ^{10}B substitution level of ~70% [E. Liarokapis (private communication)].
[9] C. Bergemann, Ph.D. thesis, University of Cambridge, 1999.
[10] D. Shoenberg, *Magnetic Oscillations in Metals* (Cambridge University Press, Cambridge, England, 1984).
[11] A. Wasserman and M. Springford, Adv. Phys. **45**, 471 (1996).
[12] H. Harima, Physica (Amsterdam) **378C–381C**, 18 (2002); and private communication.
[13] I. I. Mazin and J. Kortus, Phys. Rev. B **65**, 180510(R) (2002).
[14] H. Rosner, J. M. An, W. E. Pickett, and S.-L. Drechsler, Phys. Rev. B **66**, 024521 (2002).
[15] Note that F_7 was only predicted by one author [12], and that this work also predicts two additional frequencies close to F_3 and F_7 which arise from slight undulations of the Fermi surface.
[16] J. R. Cooper *et al.*, Physica (Amsterdam) **385C**, 75 (2003).